

The Effectiveness of using a Non-Platinum Catalyst for a Proton Exchange Membrane Fuel Cell (PEMFC)

D J. Reddy, F. d'Almaine

Durban University of Technology, Dept. of Electrical Power Engineering, Steve Biko Campus, Mansfield Road, Durban, South Africa

Abstract—The effectiveness of using a non-platinum material combination for a Proton Exchange Membrane Fuel Cell was studied. Three MEAs were characterized, two with a platinum catalyst loading of 0.1 mg/cm² and 0.3 mg/cm² and one with catalyst loading of 2 mg/cm² of silver (Ag) particles on the anode side and a combination of 1.5 mg/cm² Ag, 1.5mg/cm² ruthenium and iridium oxide on the cathode side which was purchased from FuelCelltec in the USA. Hydrogen and oxygen was applied on either side of the non-platinum MEA to provide an additional test sample (MEA 4). The active area of the cell was 9 cm². The performance of the Pt loaded PEMFC was characterized first to ensure the reliability of experimental setup and testing procedure. The tests were run at 0.5 bar at a temperature of 25 °C and 35 °C. Hydrogen and oxygen volume flow rates were varied between 19 – 95 ml/min. The best open circuit voltage achieved for MEA 3 and 4 was 0.486 V and 0.34 V respectively. A maximum current density of 15x10⁻⁶ and 50x10⁻⁶ A/cm² was achieved. The maximum power density found was 2.3x10⁻⁶ and 1.99x10⁻⁶ W/cm². The identification of the particles size and dispersion was performed by scanning electron microscope.

Keywords—Current density, power density proton exchange membrane fuel, membrane electrode assembly, polymer electrolyte fuel cell, volume flow rate.

I. INTRODUCTION

Industrialisation and the advances in technological aids to enhance the quality of life have placed enormous demands on energy sources (resultant load-shedding periods imposed in South Africa). The volatile political situation in the Middle East (major suppliers of oil) and the reality that oil resources are not an unlimited source has necessitated the practical need to explore alternate energy sources that are cost effective.

Commercialisation of PEMFC has been slow mainly due to the high cost of using Pt on the electrodes. Platinum electrodes are used due to the fast reaction kinetics which

reduce energy losses and improves cell performance [1]. Advances have been made in reducing the Pt loading from 25 mg/cm² to 0.05 mg/cm² without reducing its performance [2].

A study conducted by Howard on designing the optimal material combination for a PEMFC showed that a weight percentage combination of 60 % gold and 40 % Pt on the cathode electrode had a 66 % improvement on the maximum current density over the Pt coated cathode when tested at low temperature [3]. Although the performance of the cell improved, the cost for the performance also increased by taking into consideration the current international trading prices of gold (R471.41/gram) and Pt (R430.44/gram) as given on the 10th October 2015 [4].

Kim et al. developed a non-platinum electro-catalyst for the PEMFC which comprised of carbon supported tantalum oxide material for the cathode side of the PEMFC. Their results in terms of electrical potential was comparable to that achieved using Pt but current density reached only as high as 9 % than that of Pt [5].

Further research is required in developing a low cost material combination which will exhibit the same or better catalytic, stability and adsorption characteristics of Pt on a PEMFC. This area can provide the possibility of developing an affordable and independent power production and storage technology for the future.

II. THEORY

A polymer electrolyte hydrogen fuel cell consist of a polymer electrolyte membrane on which catalyst particles supported on carbon are applied to on either side, this is called the membrane electrode assembly (MEA). A gas diffusion layer is placed on the catalytic active area to ensure good electrical contact between the flow field plate and active catalyst area. The flow field plates have machined gas channels to transport the gases to the reaction site. End plates are used to enclose the MEA and flow field plates. Gaskets are placed between the MEA's and flow

field plates to prevent gas leaks and ensure proper sealing [6].

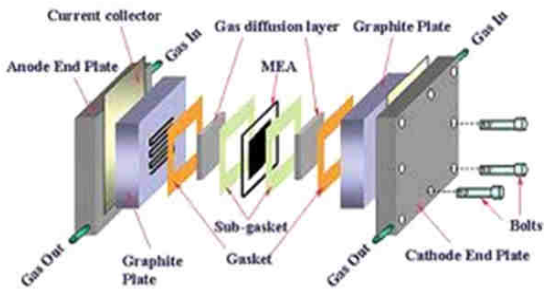
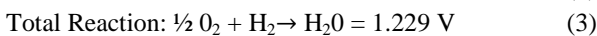
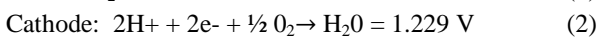


Fig. 1: Fuel cell components [7].

A fuel cell is an electrochemical energy conversion device. It directly converts chemical energy into electrical energy. Hydrogen enters the fuel cell at the anode where it is adsorbed and stripped of its electrons.



The protons move through the electrolyte and the electrons move through an external current to create electricity. Oxygen enters the fuel cell at the cathode where it combines with protons and electrons at the catalyst to form electricity and water [8].

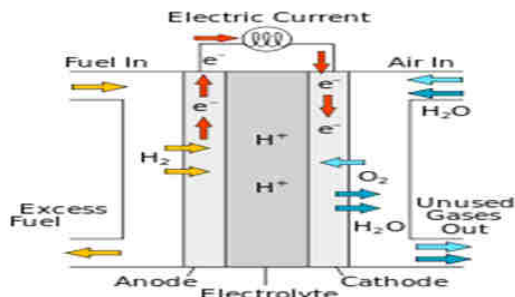


Fig. 2: Operation of PEMFC [7].

2.1 Chemical Thermodynamics

The main process of the fuel cell reactions which were described earlier is the same as the combustion of hydrogen reaction. The maximum amount of thermal energy that may be extracted from the combustion of hydrogen is determined by its heating value or enthalpy which is 286 kJ/mol at standard temperature and pressure (STP). The portion of hydrogen's higher value that can be converted to electricity in a fuel cell is called the Gibbs free energy and is equivalent to 237.34 kJ/mol [8]. This is the maximum energy input into the hydrogen fuel cell. The remaining 46.68 kJ/mol that is converted into heat is the entropy of

the chemical reaction [9]. The theoretical energy required for the reaction to proceed can be expressed as follows:

$$\Delta G = \Delta H - T\Delta S \quad (4)$$

Where:

ΔG = Change in Gibbs free energy

ΔH = Enthalpy change of reaction

ΔS = Entropy change

T = Temperature in Kelvin

The maximum theoretical voltage of a cell is referred to as the reversible voltage ($V_{\text{reversible}}$) which can be obtained using Gibbs free energy. The reversible voltage for a hydrogen reaction that produces 2 electrons per molecule is shown below [6]:

$$V_{\text{reversible}} = - \Delta G / 2F \quad (5)$$

$$V_{\text{reversible}} = - (237200) / 2(96485) \quad (6)$$

$$V_{\text{reversible}} = 1.229 \text{ V} \quad (7)$$

Where :

$V_{\text{reversible}}$ = reversible voltage of a hydrogen fuel cell at standard temperature.

ΔG = change in Gibbs free energy of formation per mole.

F = Faradays constant (96485, 3 C.mol⁻¹)

2.2 Overpotentials

Losses of voltage below open circuit voltage are usually called over potentials. Those losses can be represented on an IV curve called a polarization curve which illustrates the overall performance of a fuel cell.

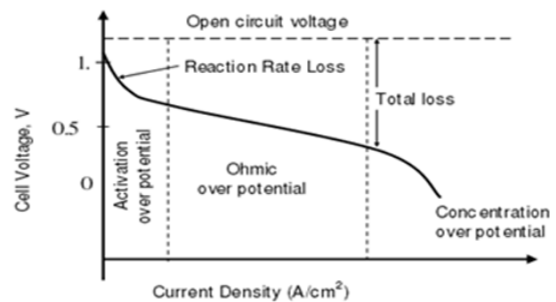


Fig. 3: Polarization Curve [10].

The three main regions depicted above correspond to the three primary regions of over potentials in the polarisation curve:

2.2.1 Activation over potential: Activation over potential refers to the amount of voltage difference from equilibrium needed to start the electro chemical reaction. The sharp drops in voltage at low current densities (1 to 100 mA/cm²) are due to activation over potential. Activation over potentials occur at both the anode and the cathode, however there is a higher activation over potential at the cathode due to the sluggish oxygen reduction reaction, which implies

that the reaction at the cathode is much slower than the reaction at the anode [11]. The anode and cathode activation losses can be calculated using equation below:

$$\Delta V_{\text{activation}} = \left(\frac{RT}{aF}\right) \ln\left(\frac{i}{i_{0,\text{anode}}}\right) + \left(\frac{RT}{aF}\right) \ln\left(\frac{i}{i_{0,\text{cathode}}}\right) \quad (8)$$

Where:

$\Delta V_{\text{activation}}$ = Activation energy losses

n = Number of electrons

F = Faraday's constant = 96400 C/mol

a = Charge transfer coefficient

i = Operating current density (mA/cm²)

i_{0, anode} = Exchange current density at the anode (mA/cm²)

i_{0, cathode} = Exchange current density at the anode (mA/cm²)

R = Gas constant = 8.314 J/mol*K

T = Temperature in Kelvin = 298 K at 25 °C

(8) above shows that by increasing the exchange current density the electrodes become more active, which reduces the amount of activation energy required to start the reactions described earlier and also increases the net output current [6][8].

2.2.2 Ohmic over potential: Ohmic losses occur at intermediate current densities (100 to 500 mA/cm²) and is represented by the straight portion on Figure 11 following the activation over potential region. Loss in voltage in this region is due to the resistance to the flow of electrons through the electrically conductive fuel cell components (R_{elec}) and to the flow of ions through the membrane (R_{ionic}) [6] [8].

$$V_{\text{ohmic}} = iR_{\text{ohmic}} = I (R_{\text{elec}} + R_{\text{ionic}}) \quad (9)$$

The electrical contact resistance is constant with respect to current and temperature. The ionic resistance is dependent on the water concentration and temperature of the membrane [6] [8].

2.2.3 Concentration over potential: Concentration losses occur at high current densities (*i* > 500 mA/cm²) following the ohmic overpotential region. The fast drops in voltage are due to the depletion of reactants at high current densities which causes rapid voltage loss. The current density at which the reactant concentration reaches zero at the catalyst surface is limiting current (I_L). Limiting current density only has an effect at high current densities. Operating the fuel cell at high current densities will not make sense as the maximum power can be reached at lower current density and higher potential. Generally fuel cells are operated at intermediate current densities [6] [8].

$$\Delta V_{\text{concentration}} = \quad (10)$$

Combing the above mentioned over potentials an expression for the operating voltage can be expressed in the following manner:

$$V_{\text{irreversible}} = V_{\text{activation}} + V_{\text{ohmic}} + V_{\text{concentration}} \quad (11)$$

$$V_{\text{cell}} = V_{\text{reversible}} - (V_{\text{activation}} + V_{\text{ohmic}} + V_{\text{concentration}}) \quad (12)$$

III. TEST CELL

The test cell consisted of a membrane electrode assembly with an active area of 9cm², comprised of Nafion 115 and a gas diffusion layer made of carbon cloth. The catalyst loading on each MEA are shown in TABLE 1.

Table 1: Type of catalyst and loading.

MEA	Anode	Cathode	Loading on anode (mg/cm ²)	Loading on cathode (mg/cm ²)
1	Pt	Pt	0.1	0.1
2	Pt	Pt	0.3	0.3
3	Ag	Ag + IrRuOx	2	1.5 + 1.5
4	Ag + IrRuOx	Ag	1.5 + 1.5	2

In order to improve the membrane proton conductivity and catalyst performance each MEA was soaked in de-ionised water for up to 100 hours before being assembled in the fuel cell [12-16].

Each MEA was placed between two flow field plates with attached gas diffusion layers. A silicone gasket was placed on the inside face of the end plates to prevent gas leaking and separate the end plate from the flow field plate. The two end plates with attached silicone gaskets were then placed against the flow field plates to enclose the fuel cell. The MEA and flow field plates were now enclosed by the two end plates. Both end plates were held together with eight bolts with washers and nuts. The nuts were first hand tightened to ensure the end plates were aligned parallel to each other. The bolts were then tightened to a torque of 3 Nm.

3.1 Experimental Setup

The test station to characterize the test cell performance was situated under a vacuum and with an extraction fan operating to ensure safety when working with hydrogen gas. Flashback arrestors were already installed on both oxygen and hydrogen cylinders as additional safety requirements in case of an explosion in either of the gas feed lines. Certified hydrogen and oxygen piping was used for connections from the pressure regulator to the mass flow controllers and humidification unit. The piping diameter was reduced to 4

mm and used flexible piping to connect to the inlets of the test cell. The mass flow controllers were manually set using the pilot interface. The humidification units to humidify the reactant gases to the test cell had to be manufactured as commercially available units were not designed to withstand pressure above atmospheric. The unit has a capacity of 2 L which was filled with de-ionized water to a volume of 1.5 L, which allowed gases to be bubbled, through at high flow rates without water spilling out.

A variable resistor with operating range of 0.1 -0 K Ω was used as the load and varied to alter the load current and voltage. A heating plate with a temperature range 0 -200 °C was used to increase the cell temperature to the required value for testing. The results displayed on the multi-meters for current, voltage and temperature were manually recorded.



Fig. 4: Experimental setup and equipment.

3.2 MEA Activation

Two operating procedures were developed: One for no - load, and the other for varying load conditions. Under no - load conditions the fuel cell (MEA 1, 2, 3) was run for 20 minutes before results were taken. Under varying load conditions, the fuel cell (MEA1, 2) was loaded for 1 hour (30 min at 500 mV and 30 min at 400 mV). MEA 3 was also run for 1 hour (30 min at 200 mV and 30 min at 300 mV) [12-16]. These voltages were selected as they are within the operational voltage range of the MEA's being investigated. The MEAs were then fully characterised by varying the load from 0.1-1 K Ω and results recorded to plot the polarisation curve. Two minute intervals were allowed before a set of readings were recorded. After this characterisation sequence the cycle was complete. This cycle was repeated twice to observe any improvement in performance. It was noted that when the cell was run immediately after the first cycle that there was a slight improvement in performance.

3.3 Experimental Procedure

- Switch on MFC and set required gas flow rates.
- Switch on hydrogen generator at set pressure to 0.5 bar.
- Open oxygen cylinder valve and set pressure to 0.5 bar.
- Run the cell for 30 minutes under open circuit condition.
- Connect variable resistor.
- Run cell under varying load setting and record voltage and current values.

IV. EXPERIMENTAL RESULTS AND DISCUSSION

4.1 Open Circuit Voltage

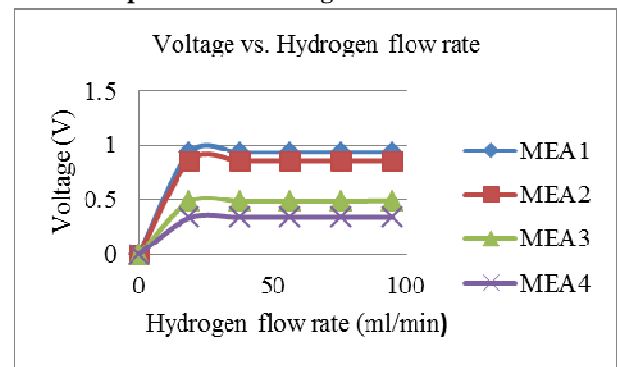


Fig. 5: MEA 1 vs. MEA 2 vs. MEA 3 vs. MEA 4, open circuit voltage, varying H₂, 38 ml/min O₂.

The voltages recorded and displayed were taken after a 20 minute time interval. The initial temperature was approximately 25 °C. The temperature measured from the current collector plate after 20 minutes was approximately 26.5 °C.

It was noted that the initial open circuit voltage was slightly higher than that recorded after 20 minutes. This was expected according to (5) as increasing temperatures reduces the amount of Gibbs free energy which causes the slight decrease in open circuit voltage.

The open circuit voltages of the MEA's improved slightly as the reactant flow rates were increased. However it was observed that not all the reactants were being utilized. The outlet for the reactants was placed in a water reservoir to confirm this. This suggests that fuel cells can be operated at reasonably higher flow rates to improve its open circuit voltage performance provided the exhaust reactants are recirculated into the cell so that the fuel utilization efficiency is improved.

The voltage difference of between MEA 1 and 2 is due to the different catalyst loading for the two MEA's. Lowering

of the platinum loading appears to affect the open circuit voltage. This could be as a result of less active reaction sites for reactants to react with.

The poor open circuit voltage of MEA 3 and 4 to the platinum loaded MEA's can be attributed to the use of a cheaper material with poor catalytic properties. The relatively poor catalytic properties of these materials adsorb reactants strongly thus requiring more energy for the surface reaction to occur.

4.2 Current Density

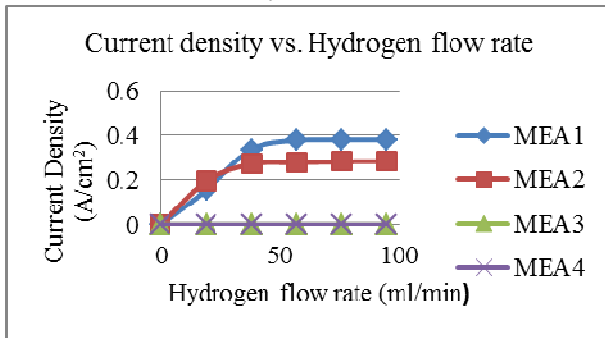


Fig. 6: MEA 1 vs. MEA 2 vs. MEA 3 vs. MEA 4, current density, varying H_2 , O_2 38 ml/min.

The maximum current density for MEA1, 2, 3 and 4 were achieved when the highest flow rates were applied. This is due to more reactants being present at the reaction sites. Increasing reactant flow rate increases the reactant concentration at active catalyst sites thereby increasing the current density. However it can be seen in Fig. 6 as the maximum current density is approached at a high flow rate, further increases in volume flow rate does not increase the current density. This shows that most of the active reaction zones are being utilized and that maximum current density is approached. MEA 1, 2, 3, 4 delivered a maximum of current density of 0.3816, 0.284, 50×10^{-6} and 55×10^{-6} A/cm² respectively. Due to the porosity of the catalyst surface there is a possibility that the maximum current density was not reached.

The 10.69 % difference in current density between MEA 1 and 2 at the highest flow rate is due to the increased platinum loading on MEA 1. Increasing the Pt loading increases the number of reaction sites available for the reactants to react with thus increasing the output current. Increasing catalyst loading also increases the exchange current densities and increases the net current generated as shown above.

Poor current densities were achieved with MEA 3 and 4. Further increases in flow rate did not improve from its initial current density at low flow rates. It was noted that the current density initially peaked 133.3×10^{-6} A/cm² for MEA

3 and 247.8×10^{-6} A/cm² for MEA 4 and then slowly decreased whilst maintaining a constant reactant flow rate. The final value recorded and provided was taken after 2 hours. The slow decrease in current density could be due to the possible formation of oxides on the catalyst surface, thus reducing the number of active sites for the reactants to react with, which significantly reduced the output current.

4.3 Polarization Curve

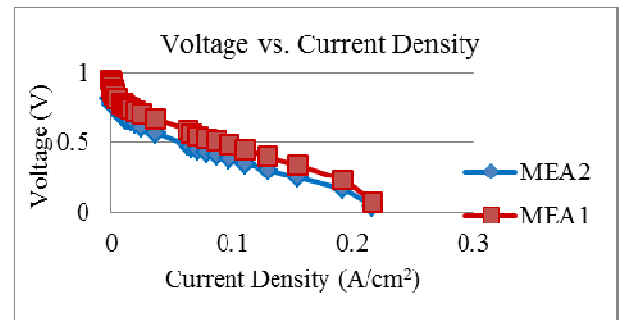


Fig. 7: MEA 1 vs. MEA 2, polarization curve at 25 °C, H_2 19 ml/min, O_2 38 ml/min.

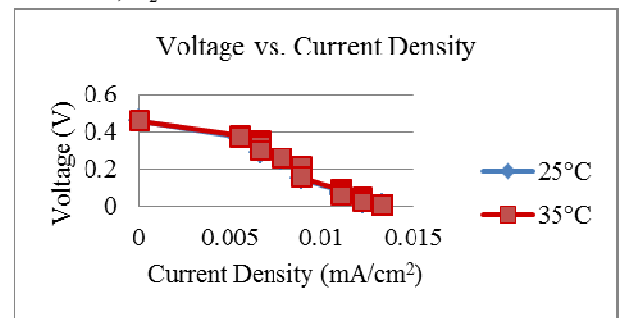


Fig. 8: MEA 3, polarization curve at 25 °C and 35 °C, H_2 19 ml/min, O_2 38 ml/min.

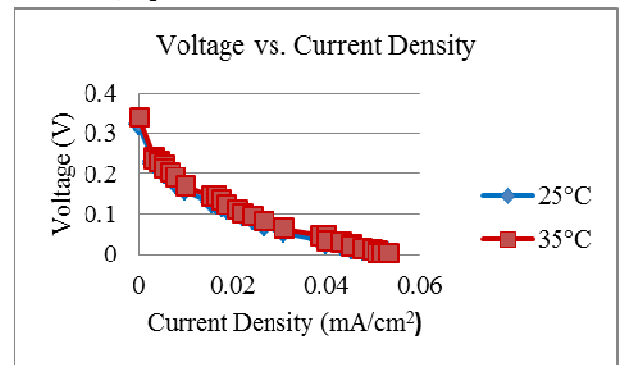


Fig. 9: MEA 4, polarization curve at 25 °C and 35 °C, H_2 19 ml/min, O_2 38 ml/min.

Voltage vs. current density plots were recorded at a constant hydrogen flow rate of 19 ml/min and oxygen flow rate of 38 ml/min at 25 °C and 35 °C. It can be seen from Fig. 7- 9 that a slight performance gain was achieved when the temperature was increased.

The low current density region shows a sharp drop in potential, this is the activation energy required to start the reaction. Increasing temperature shows a decrease in the amount of activation losses which meant the reaction was able to precede at a faster rate hence less loss of potential from reaction kinetics. Increasing temperature also increases exchange current density which decreases the activation over potential.

The over potential losses in the intermediate current density region is attributed to ohmic losses which increase with current and temperature see (9). At higher temperature ohmic losses are increased due to membrane drying. Supplying humidified gases improves membrane conductivity which allows protons to be conducted more easily through the membrane and decrease its resistance hence the decrease in ohmic losses in the intermediate region.

The high current density region shows a rapid decrease in cell potential due to concentration over potential which is expected as a result of reactant consumption at the catalyst site exceeding the rate of reactant diffusion. At higher temperature there is a decrease in concentration over potential. Overall the cell performance increased at higher temperatures due to a decrease in losses.

4.4 Power Density

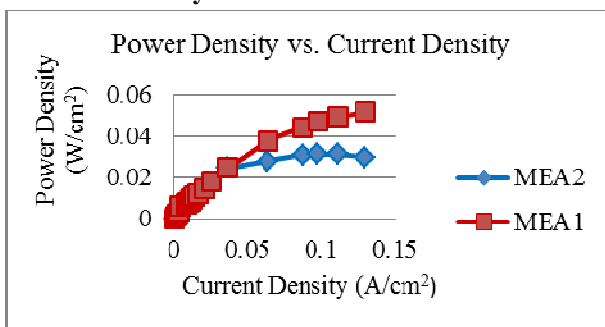


Fig. 10: MEA 1 vs. MEA 2, maximum power density at 25 °C, H₂ 19 ml/min, O₂ 38 ml/min.

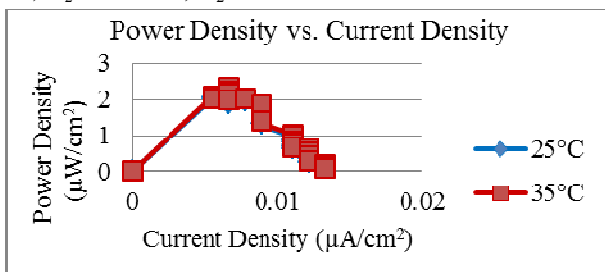


Fig. 11: MEA 3, maximum power density at 25 °C and 35 °C, H₂ 19 ml/min, O₂ 38 ml/min.

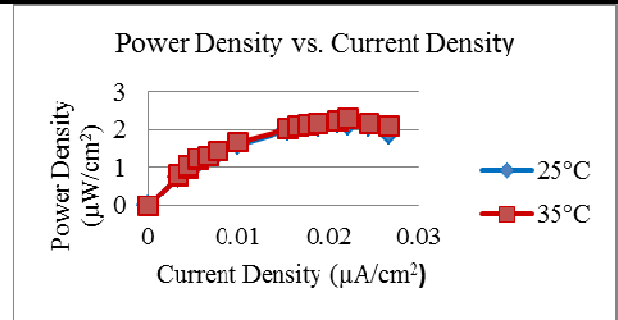


Fig. 12: MEA 4, maximum power density at 25 °C and 35 °C, H₂ 19 ml/min, O₂ 38 ml/min.

The plots of power density vs current density are shown in Fig. 10- 12. It can be seen that the power density has a fairly linear relationship with current density up to the maximum power point, further increase in current shows a drop in cell power density and this could be due to insufficient supply of hydrogen to the active area surface.

MEA 1, 2, 3 and 4 delivered a maximum power density of 0.05, 0.038, 2.3x10⁻⁶, 1.99x10⁻⁶ W/cm² respectively at 25 °C. The 10 °C increase in temperature increased the power delivered by the MEAs to 0.06, 0.0488, 2.342x10⁻⁶, 2.212x10⁻⁶ W/cm². The slight increase in power density for the MEAs for a 10 °C temperature increase was expected. This is due to a higher current density being achieved with a lower overpotential as the reaction kinetics increased.

The significant decrease in power density for MEA 3 and 4 compared to MEA 1 and 2 is due to the poor exchange current density of the material. This results in higher over potentials and low net output current due to reaction proceeding at a slow rate and the possible formation of oxides on the catalyst surface.

The 22.6 % difference in maximum power density between MEA 1 and 2 at 25 °C is due to the higher Pt loading on MEA1 as discussed earlier which increases the exchange current density and current output at a given potential.

4.5 Scanning Electron Microscope

The images below show the particle morphologies and a fairly uniform dispersion onto the Nafion membrane. The particle size measured from the SEM image was 6.6µm.

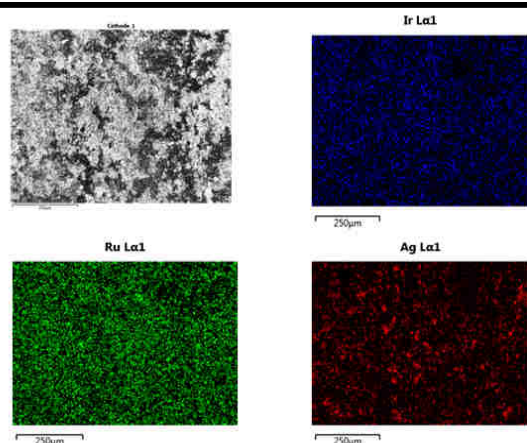


Fig. 13: Size and dispersion of catalyst particles on the anode and cathode.

V. CONCLUSION

It had been hypothesized that using a low cost material combination for the catalyst layer would produce an acceptable amount of electrical energy. The maximum power density results obtained with the Pt catalyst were comparable to those achieved by other researchers which ensured that the test cell was well developed and that the experimental setup and operating parameters settings were correct. The custom made non Pt loaded catalyst performance was found to perform poorly against the commercial Pt loaded catalyst due to the much stronger adsorption and poor stability characteristics of the material combination considered. The open circuit voltage was expected however the poor current density achieved needed further investigation. Characterization of the catalyst layer using appropriate testing methods are required to confirm the possible presence of oxides on the catalyst surface which could significantly reduce the number of reaction zones thus decreasing the net current generated in this study. Investigations into the fine tuning of the electronic configurations of materials are also required to achieve the ideal catalyst.

REFERENCES

- [1] Appleby, A. J and Foulkes F. R, (1993), Fuel cell handbook, Krieger Publishing Co, Florida.
- [2] Daouda Fofana, Sadesh Kumar Natarajan, Pierre Bénard, and Jean Hamelin, 'High Performance PEM Fuel Cell with Low Platinum Loading at the Cathode Using Magnetron Sputter Deposition, ISRN Electrochemistry, Volume 2013 (2013), Article ID 174834, 6 pages, 25 November 2012.
- [3] Elizabeth Stockton Howard, 'The Design of Optimal Material Combinations for the Membrane Electrode Assembly of a Proton Exchange Membrane Fuel Cell', Bachelor of Science in Engineering Degree, Princeton University, 2006.
- [4] www.infomine.com, accessed 10 October 2015.
- [5] JY Kim, T Oh, Y Shin, J Bonnett, K Scott Weil, 'A novel non platinum group electrocatalyst for the PEM cell application, International journal of hydrogen energy, 2010.
- [6] Frano Barbir, 'PEM Fuel Cells: Theory and Practice', United States of America, Elsevier, 2005.
- [7] Jianlu Zhang, Huamin Zhang, Jinfeng Wu, Juijun Zhang, 'PEM Fuel Testing and Diagnosis', Elsevier Publishing 2013.
- [8] Colleen Spiegel, 'Designing and Building Fuel Cells', 1st ed. New York, NY, McGraw-Hill, 2007.
- [9] James Larminie, Andrew Dicks, 'Fuel Cell Systems Explained', second edition, John Wiley and Sons, The Atrium, Southern Gate, Chichester, West Sussex PO198SQ, England.
- [10] Doddathimmaiah, A. K. 2006. 'The use of PEM unitised regenerative fuel cells in solar-hydrogen systems for remote area power supply'. School of Aerospace, Mechanical and Manufacturing; RMIT University.
- [11] A. Husar, S. Strahl, J. Riera, 'Experimental Characterization Methodology for the Identification of Voltage Losses of PEMFC: Applied to an Open Cathode Stack', Institut de Robòtica i Informàtica Industrial (CSIC-UPC).
- [12] US Fuel Council's Single Cell Testing Task Force, 'Single Cell Test Protocol', Washington, DC, July 13, 2006.
- [13] X.Z. Yuan, S. Zhang, J.C. Sun, H. Wang, 'A review of accelerated conditioning for a polymer electrolyte membrane fuel cell', J Power Sources, 196 (2011), pp. 9097-9106, Volume 38, Issue 23, 6 August 2013, Pages 9819-9825.
- [14] Mohammad Zhiani, Somayeh Majidi, 'Effect of MEA conditioning on PEMFC performance and EIS response under steady state condition', International Journal of Hydrogen Energy, Volume 38, Issue 23, 6 August 2013, Pages 9819-9825.
- [15] C. Yang, M. Hu, C. Wang, G. Cao, 'A three-step activation method for proton exchange membrane fuel cells', J Power Sources, 197 (2012), pp. 180-185.

- [16] Valter Bruno Reis e Silva, 'Polymer Electrolyte Membrane Fuel Cells: Activation Analysis and Operating Conditions Optimization', Doctor of Philosophy in Chemical and Biological Engineering, Porto University, August 2009.